College of Engineering
UNIVERSITY OF WISCONSIN–MADISON

Turbine Technical Design Report

2023 Collegiate Wind Competition

University of Wisconsin-Madison

WiscWind

Overall Team Lead: Michael Schmich (schmich@wisc.edu)

Team Advisor: Scott Williams (spwilliams@wisc.edu)

Faculty/Staff Advisors: Randy Jackson, Kyle Hanson, Daniel Ludois

Electrical Sub-Team	Mechanical Sub-Team	Substructure Sub-Team
Led by: Nazrie Hasan (mbhasan@wisc.edu)	Led by: Teddy Hines (thines3@wisc.edu)	Led by: Josh Delgado (jdelgado22@wisc.edu)

Table of Contents

Executive Summary

This design report outlines the technical design, manufacture, and testing of the University of Wisconsin-Madison WiscWind competition team's scale wind turbine created for the 2023 Collegiate Wind Competition. In an effort to successfully complete all testing procedures during the competition, while excelling in categories like energy efficiency and substructure design, the team chose to redesign the entire turbine and control system.

While designing the new turbine and subsystems, unique circumstances of the competition were considered such as the time constraints of turbine operation modes, the PCC voltage requirements, overall sizing of the turbine components, as well as the incident stresses during high wind speed conditions. Two turbine prototypes were built this year, one during the Fall semester to test a newly designed generator and the other during the Spring semester to improve on the lessons learned from the Fall semester trial. The first turbine was designed with the power output as a main design consideration in an effort to boost power output of the turbine over a range of 5-11 m/s. The generator designed for that turbine was oversized for the application but still produced a significant power output at a remarkable efficiency. However, following wind tunnel testing of this prototype–it was found that the large inertia of the generator steel rotors made the time to reach critical speed at each operating point far longer than allowed. Additionally, the size of the blades required to provide enough torque for the generator to operate was unconventional and inefficient. To improve on these points, a new turbine was constructed with a newly designed generator that was smaller in size, had a smaller machine constant to limit voltage, and allowed for a more efficient blade design since the generator needed less torque for efficient machine operation.

The mechanical sub-team followed standard engineering practices during the physical construction of the turbine and created a robust design. By using materials like low-carbon steel, aluminum, cast acrylic, and reinforced plastic the turbine was constructed with safety and smooth operation in mind. A new pitch head was modified from an RC helicopter to connect with the main turbine drive shaft. This pitch system utilizes two linear actuator servos to set the desired pitch at any given operating point. The turbine blades were designed using QBlade software, following many design iterations on tip speed ratio, coefficient of power, and lift-to-drag ratio. Then, the turbine blades were 3D printed in reinforced PLA and in carbon fiber reinforced PETG.

To control the turbine during different operating conditions, two arduino microcontrollers were implemented to receive and process signals from various sensor and control inputs. The controllers communicate via over-the-air RF communication to negate the need for wired connections between the electrical enclosures other than through the PCC. To operate the turbine generator most efficiently, a variable load rheostat is coupled to a servo to give the load controller a handle on the load value at any given operating point. A pitot tube was coupled with an analog differential pressure sensor to accurately read the wind speed and relay the information to the load microcontroller for it to select the optimal load.

By utilizing the software features in the C++ based Arduino architecture, instantaneous RPM reading, wind speed reading, pitch actuator control, and load control are possible. These features allowed the team to do extensive wind tunnel testing to observe the turbine's performance in each competition task. The power output characteristics and success of turbine safety controls were evident from numerous performed tests. Previous years' competitions have shown the team edge cases for the turbine controls to account for, desirable characteristics for smooth performance, and the practice to create an efficient generator.

Design Objective

The group's design objective for the 2023 Collegiate Wind Competition was to construct a small-scale wind turbine that operates similarly to a large-scale offshore wind turbine. New for this year's competition–the turbine control system was designed to be able to control the power output of the turbine past 11 m/s. To do this, a wind sensor was used in conjunction with the linear actuator pitch control to pitch the blades forward slightly past the most efficient point to slowly reduce the efficiency of the blades at each wind speed until 15 m/s. Additionally, the substructure was designed to be able to engage the sand in the sand-water tank, over last year's design which involved excavation of the sand. This was accomplished by creating an auger substructure design that could twist into the sand base rather than excavating. The control systems were designed to optimize power production at wind speeds of 5-11 m/s, act quickly on safety shutdown conditions, and maintain turbine integrity during high speeds of up to 22 m/s.

Mechanical Design & Analysis

Blades

The mechanical team chose the simulation software, QBlade, to design blades that will extract the maximum amount of power. First, various airfoils from NACA, The National Advisory Committee for Aeronautics, were simulated under the competition conditions to determine which airfoil will be able to have the highest power coefficient. Other airfoils were explored from a few different aerodynamics studies and the winning airfoil selected was the Wortmann FX 60-126. Next, using Betz correlations, the chord length and twist angle of the blade were determined by inputting different tip speed ratios. Tip speed ratios from 2 to 5 were simulated and ultimately a tip speed ratio of 3.5 was proved to have one of the highest power coefficients, while providing a good deal of structural rigidity for a 3D printed blade. A plot of power coefficient versus tip speed ratio of this optimized blade is shown in Figure A-2, with a maximum power coefficient 0.385. This blade was then 3D printed with fiber reinforced PLA and attached to the rotor hub.

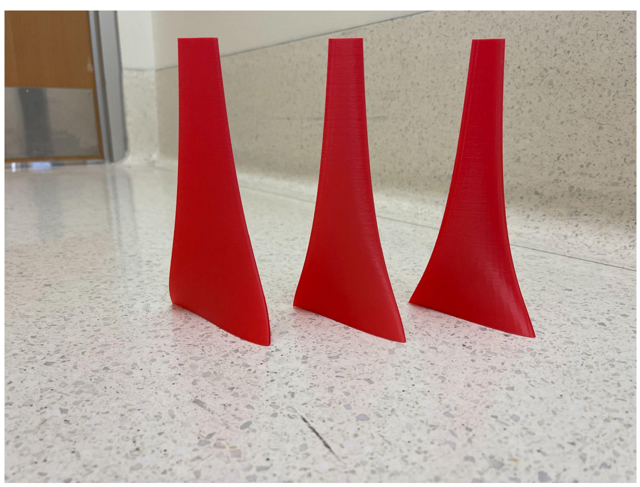

Figure 1: Prototype blades at TSR = 3.2, 3.5, 4

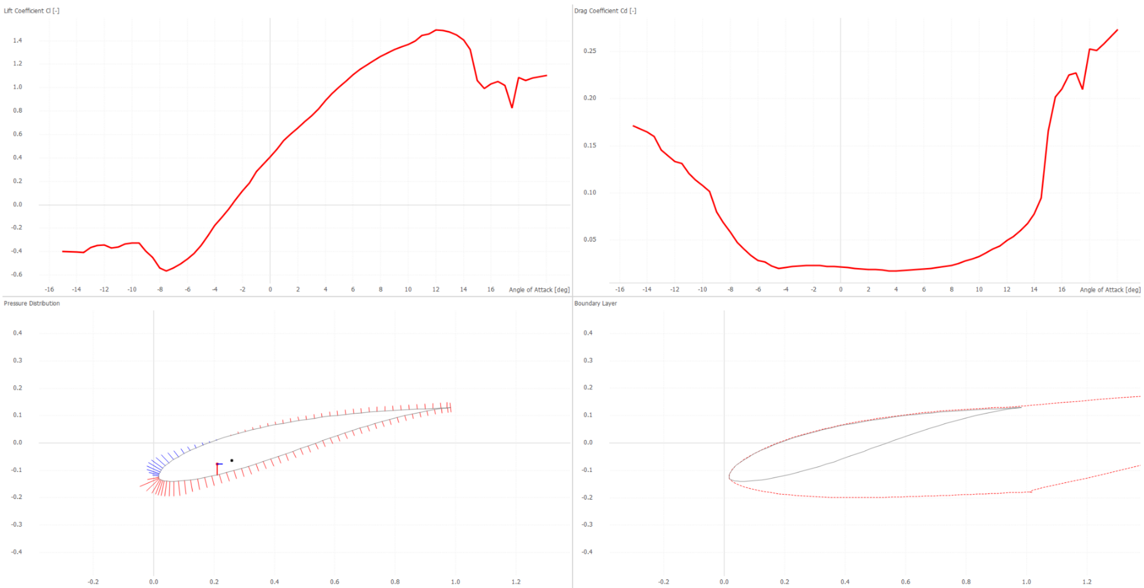

Figure 2: Lift coefficient, drag coefficient, pressure distribution, and boundary layer vs angle of attack for the Wortmann FX 60-126 airfoil in QBlade.

Once the proper airfoil was decided, the power coefficient needed to be maximized.The team learned that if the Reynolds number was adjusted to be around 50,000-100,000 and Prandtl tip losses were taken into account, the value of the power coefficient was much more accurate. The power coefficient tells you how efficiently the turbine converts the energy in the wind into mechanical energy. Since the airfoil was set, the size and shape of the airfoil could be adjusted by inputting what tip speed ratio the blade should be optimized at. Taking in this tip speed ratio, QBlade used betz correlations to produce the ideal blade by adjusting chord length, size, and twist. After testing a variety of tip speed ratios, it was found that the blade could reach a maximum power coefficient of 0.38 at an optimized tip speed ratio value of 3.7. Below in Figure 2 is the Qblade plot of the power coefficient vs tip speed ratio for the Wortmann FX 60-126 airfoil at a tip speed ratio of 3.5.

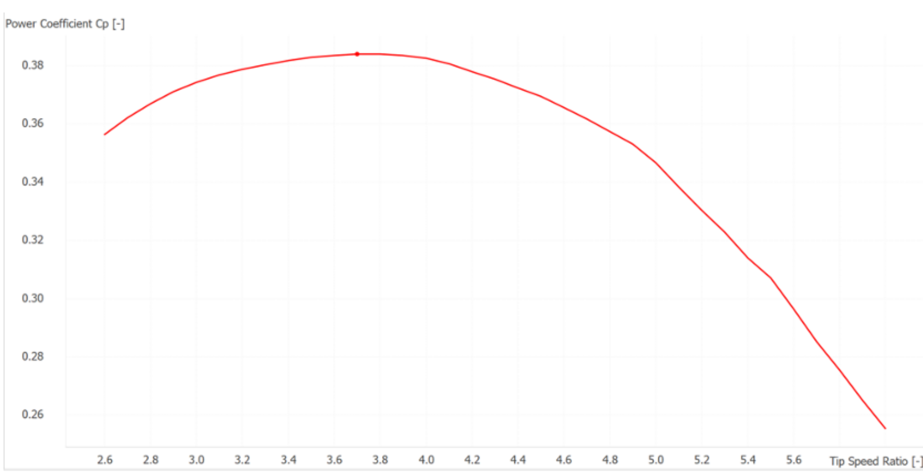

Figure 3: Power coefficient vs tip speed ratio of the Wortmann FX 60-126 airfoil at an optimized tip speed ratio of 3.5

Figure 2 shows that the maximum power coefficient of 0.38 occurs at a tip speed ratio of 3.7. Although, the power coefficients of the blades optimized for a tip speed ratio from 3.3-3.7 all had a maximum power coefficient of near 0.38. Therefore three different sets of blades were printed: blades with a tip speed ratio of 3.3, 3.5, and 3.7. All blades had a length of 19 cm, since that was the maximum size allowable accounting for the 3.5 cm distance to the center of the pitch control head. These blades were designed in QBlade, adjusted to fit the rotor in SOLIDWORKS, then printed with PLA in the WiscWind 3D printer.

Pitch Control

The pitch control system consists of two linear servo motors, a coupling mechanism, and RC helicopter rotor head. An issue with the rotor head was that it needed to be restricted to one degree of freedom to solely control pitching, not tilting, and only move axially along the shaft. This was accomplished by removing the ball bearing in the swash plate and press-fitting a cylinder bushing in instead. To couple the swash plate to the actuators, a 3D printed form was designed that surrounded the swash plate and screwed into the plate at the control rods. Three iterations of this coupler were tested until the current design was selected. This coupler is joined to the actuators through metal rods that extend through the coupler and are offset above and below the rotor shaft. The reason these shafts extend through the coupler and are offset is to minimize a bending moment created on the shaft when the actuators are engaged.

One major issue that was encountered with the first prototype was that linear stepper motors were used instead of servo motors. The stepper motors didn't have an absolute positioning system which made pitch control testing difficult as the position was only incremental from the position the actuators were at when connected to power. Associated with this, the stepper motors would error out and need to be reset if incremented beyond their available path on the shaft and collided with the rotor head. The second iteration of motors were linear servo motors and had absolute positioning which was needed for the control system implemented. The new servo actuators were slightly larger than on the first prototype and were too large for the existing front bearing block, so shims needed to be attached to the bearing block with new holes drilled and new mounting brackets designed and 3D printed.

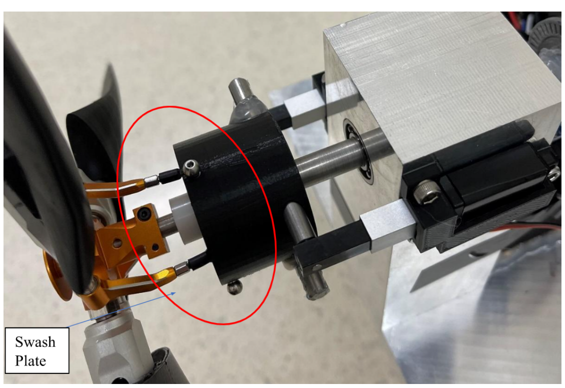

Figure 4: Pitch control system from first prototype

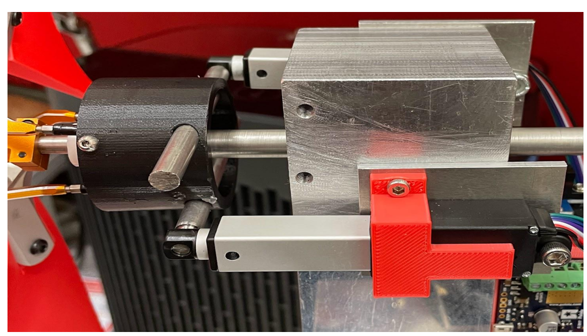

Figure 5: Revised actuators and mounting with second prototype

Turbine Mechanical Loading

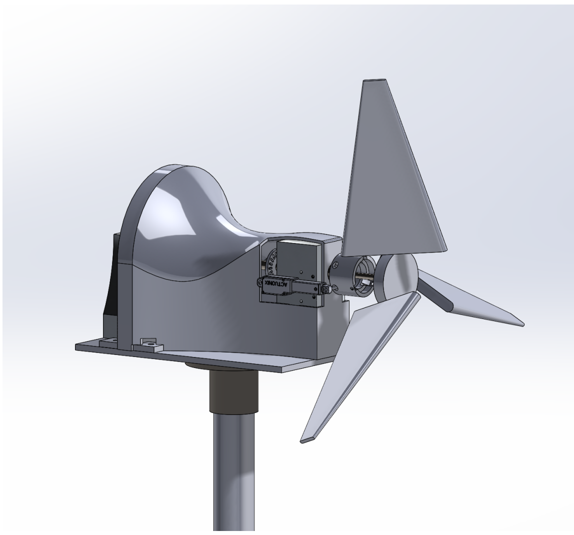

Figure 6: Full SOLIDWORKS model of turbine with Nacelle

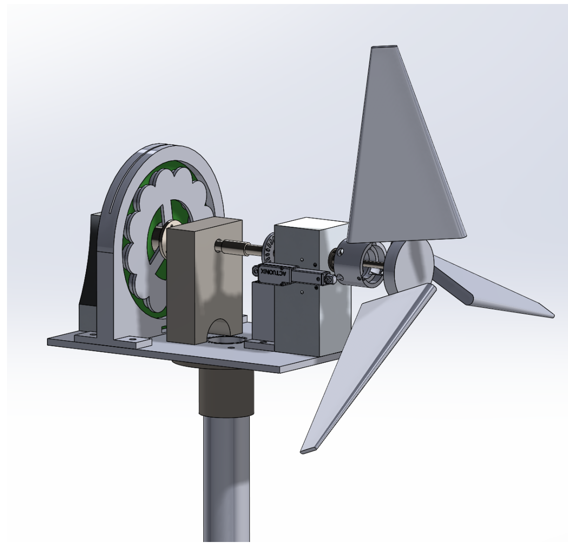

Figure 7: SOLIDWORKS model of internal turbine components

A main issue with last year's turbine is that the linear actuators holding the blades in place were not always strong enough to repel against the drag force from the incoming wind. Therefore this year we made a strong point to ensure strong enough linear actuators were ordered. According to the substructure analysis, the maximum drag force from the incoming wind was about 47 Newtons. The specifications from the desired actuators from Acutonix listed a maximum load of 80 Newtons. Since our design has two actuators holding the blades, this gave us a safety factor of 3.4. This was deemed a high enough safety factor and actuators did hold up when tested in the wind tunnel at 22 [m/s].

For the bearing load calculations, the rear two bearings equally support the weight of the generator assembly and the front bearing supports the weight of the rotor head, blades, and drive shaft. For the rear bearings, the load from the generator assembly which includes the generator shaft, rotors, magnets, and flanges is 35N. Since the generator load is split between the two rear bearings, each of those bearings experiences a load of 17.5N. The bearings used are each rated for 1335N loads so this provides a safety factor of 76.29 for each of the read bearings. For the front bearing, the load on that bearing from the drive shaft, rotor head, and blades is 13.35N. With the bearing rating of 1335N, the factor of safety for the front bearing is 100.

The bending load on the generator shaft is the weight of the rotors, the magnets, and the flanges which is 26.69N. The generator shaft is made from stainless steel which has a very high rated bending stress of about 500MPa. Since the shaft is ⅜" in diameter, the rated bending load of this shaft is 41161. This rated load gives a safety factor of 1542 which is very high but expected due to the fact that stainless steel is very strong.

Substructure Design & Analysis

Using information gained from the previous year's competition, the substructure sub-team designed, prototyped, 3D-printed, and tested many different ideas throughout the year. The goal for the substructure team was to maximize the counter moment produced by the substructure to avoid the structure from tipping at higher wind speeds. First the team needed to determine the necessary counter moment required by the substructure to keep the turbine upright and prevent shifting. After adjustments to the design of the turbine the substructure team modified the necessary torque required to keep the turbine upright. The substructure design team calculated the theoretical drag force created by the wind. Using equation [1], the team found that the maximum drag at the turbine height due to the rotor was a force of about 46.9 N.

$$F_{D_{max}} = \frac{1}{2}\rho A c_{D_{max}} V_{max}^2 \qquad [1]$$

$F_{D_{max}}$ = Maximum Drag Force [N] ρ = Density of air [1.293 $\frac{kg}{m^3}$] $c_{D_{max}}$= Drag coefficient

A = Projected area [m^2] V_{max} = Maximum Wind Speed [$\frac{m}{s}$]

Next the force of the wind on the pipe was calculated using the same equation. This force was found to be a little over 2 N. Using the maximum distances, the total moment at the substructure was calculated to be around 48 N-m. Using this calculation, the team designed several structures capable of creating a large enough counter moment in the sand.

Designs and Civil Analysis

After developing several designs and receiving feedback from the judges, the team decided to pursue an auger-based design. The team's goal was to use the pressure of the sand and the weight of the turbine to provide the greatest possible counter-moment. To do this, the team decided to use plates with large surface areas perpendicular to the direction of wind to capture the lateral pressure of sand and provide a counterweight. The natural geometry of the auger also allows the weight of sand to be captured by the flanges, contributing to the counterweight. The team determined that the farther the tipping point is from the center of the substructure, the larger the provided counter-moment. Once these factors were determined, the team began to redesign new substructures. The first main design is seen below in figures 8 and 9.

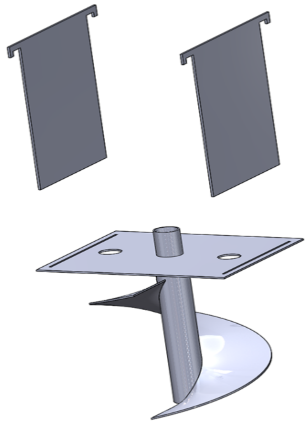

Figure 8: Initial substructure SOLIDWORKS design

Figure 9: First substructure iteration

This model features a 10” diameter auger with a 8” pitch to be rotated into the sand until the top plate becomes flush with the sand surface. To maximize the surface area in the sand without violating the excavation rule, the team designed vertical slats that are pushed vertically into the sand through slots in the substructure top. These slats are installed after the auger is twisted into its position in the sand to comply with the rules. These vertical slats provided a large surface area that is perpendicular to the wind to provide a large counter-moment in the sand. These slots are present on both main substructure designs as they proved to be a crucial factor in the strength and stability of the substructure. Initial testing suggested that the original auger’s pitch was too large, making the flanges prone to slipping on the sand and restricting the weight available for capture by the substructure. To fix this issue, a second auger was purchased with a lower, 4” pitch. As testing proceeded, the team hypothesized that installing the slats at slight angles may provide a larger counter moment than vertical orientations. These angled plates would force more sand to be moved as the substructure attempted to tip. After modifying the top plate of the substructure and designing the holes to accommodate angled slat installations, the team resumed data collection. As seen in Table 1 below, when the side plates were installed at the maximum allowable angle, the auger outperformed the other designs.

Table 1. Failure Torque at various side plate orientations

	Measured Torque at Failure(N-m)		
Substructure	Auger Component Only	Auger with Side Plates	Auger with Angled Side Plates
10” Diameter Auger Design	9.8	16.7	18.6
8” Diameter Auger Design	26.46	45.08	49.2

While the new auger improved the overall structural integrity, the factor of safety was undesirable and introduced potential failure at high wind speeds. To combat this, a slot-in mechanism for two 5kg weights was created on the front facing side, significantly improving the weight distribution of the entire system. With this change, the counter moment induced significantly increased the structures ability to resist large torques and significantly limited the movement of the system which would affect the turbine's performance. With the additional weights added, the substructure was able to reach a torque of 75.5 N-m before any significant movement. This gave the team a factor of Safety of 1.6 which was desirable. This final design can be seen below in SOLIDWORKS (Figure 10) and after manufacturing with one of the two weights (Figure 11).

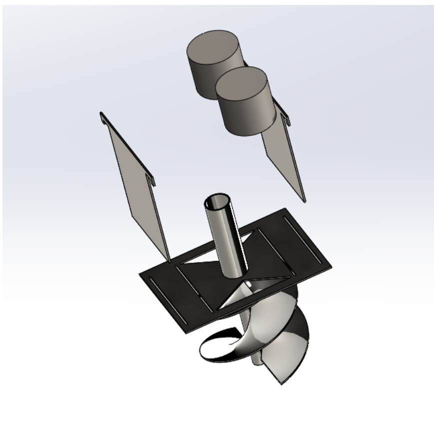

Figure 10: Final SOLIDWORKS design of substructure

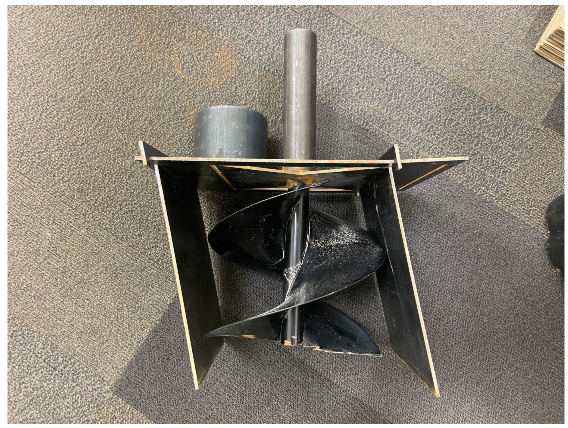

Figure 11: Final iteration of substructure

Testing Setup

In order to properly simulate the correct stresses and record data to gauge the substructure's performance, the team purchased equipment capable of recreating the setup used at competition. The team purchased a large 30" x 20" x 15" tub and 200 lbs of sand, placed the sand in the bucket, and covered the sand with water to fully recreate the competition conditions. Next, the team installed the substructure into the sand and inserted a long slender rod to recreate the torque generated by the high-speed winds. To measure the torque applied, a force sensor was latched onto the rod using a hook and was pulled at a steady rate until the substructure tilted out of the sand. Reading the force sensors peak value gave the peak force required to cause the substructure to fail.

Manufacturing

To manufacture the substructures several different methods are utilized. As the team decided on an Auger based design the team decided that the quickest and most cost-efficient process would be to purchase a large auger made of completely ferrous materials online. Once the auger arrived, it was cut down in length using an angle grinder. Using an angle grinder allowed the team to accurately cut through the steel of the auger to the correct length despite the unique shape. To manufacture the top plates of the augers and slats, a waterjet cutting machine was used. The team chose the waterjet tool as it provided a precision cut at a low cost. The cuts for the top plates needed to be precise as the holes for the vertical slats needed to be a tight fit to not allow for the turbine to move. After the components were designed, the substructure was welded to the top plate. An additional stem was welded onto the top of the turbine with a 1.2” diameter hole to allow for the electrical cable to go into the stem.

Installation Method

After constructing the prototype and testing for performance, a plan was developed to install the substructure according to the competition rules. Because the installation cannot involve contact with the water, a tool was designed and built to facilitate easy rotation of the auger into the sand from a fixed distance above the substructure top. The top plate above the auger used to guide the side slats has triangular holes originally made to reduce weight. The team took advantage of these triangular holes by purchasing a 1-¼” diameter PVC pipe and two tee connectors. A section of pipe was cut to a length matching the distance between the triangular holes, and tees were attached on either end. Two more sections of pipe were cut to be equal lengths longer than the central shaft protruding from the substructure, and were fitted into the tee connector. This tool, shown below in figure 12, allows for the rotational sinking of the substructure from a height, avoiding contact with the water.

Figure 12: PVC tool used to install substructure

Next, tools were constructed to facilitate the insertion of the slats into the top plate. Using another section of PVC pipe, a notch wider than the width of the ⅛” steel slats was cut into the end. These notched pipes can be placed on the top slat edge after being aligned with the top plate slots to drive the slats into the sand. A rubber mallet will be used to aid the driving of the slats. Once the slats are inserted, the inner slots in the headwind direction are utilized to secure the weights on the top plate of the substructure. Finally, for removal, pliers will be used for the side slats, and the custom PVC tool will be used for twisting the substructure back out of the sand.

Electrical Systems

Electro-Mechanical Energy Conversion

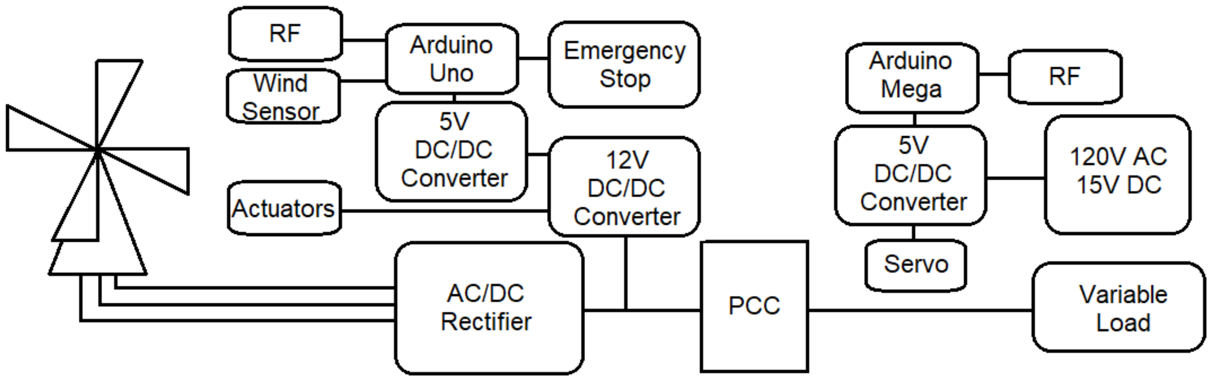

Figure 13: Electrical one-line diagram of turbine and load sides of the PCC

The wind turbine electronics enclosure can be seen below. The enclosure was constructed with the abilities to provide power to the turbine side electronics via a 12V and 5V bus coming from two DC-DC converters. The turbine side electrical components are controlled by an Arduino Uno R3, which handles the sensor inputs from the e-stop button, rotary encoder, pitch actuators, wind sensor, and RF transmitters. New for this year, RF sensor modules are used to communicate between the two electrical enclosures wirelessly. This method of communication was tested via writing and receiving from both enclosures under a variety of circumstances, each time performing as expected and outputting the correct data on the receiver side. The braking code involving the e-stop button was tested in our office and in the wind tunnel, working both times as successfully initiating a back feed of power from the load enclosure to the turbine electronics for braking, then turning off once the braking is reversed.

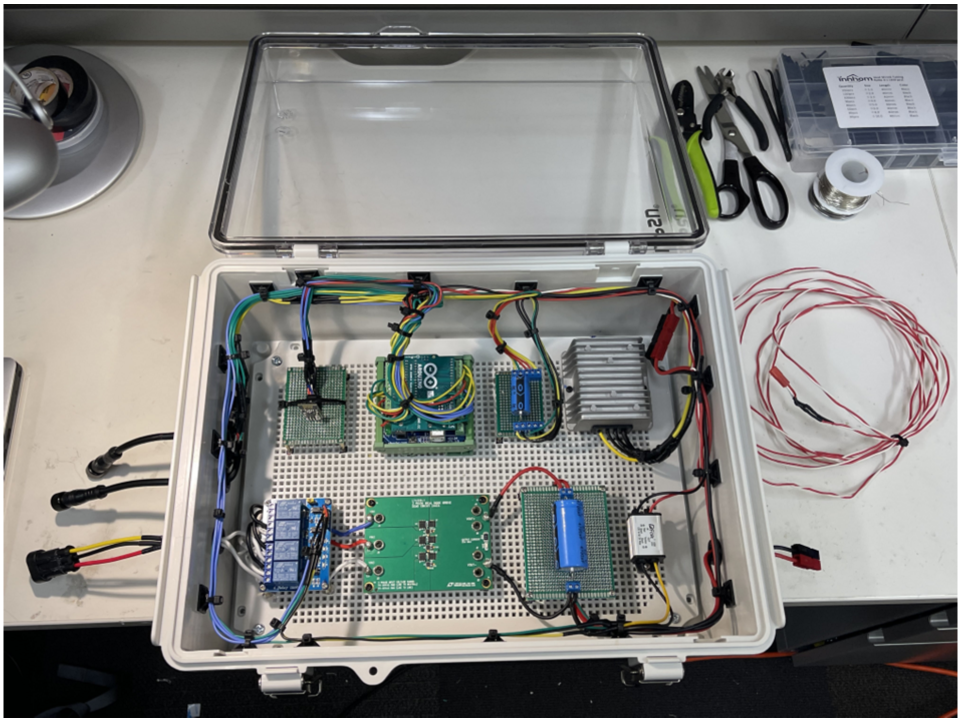

Figure 14: Turbine-Side Electronics Enclosure

A thermal anemometer was utilized with a mode averaging method on the Arduino to try to provide a stable reading of the wind speed, but ultimately was scrapped for a pitot tube with an analog differential pressure sensor for greater precision and consistency. The pitot tube was mounted toward the bottom of the competition stem to provide enough room so as to not allow the wind dispersion from the spinning rotor to affect the wind speed measurement.

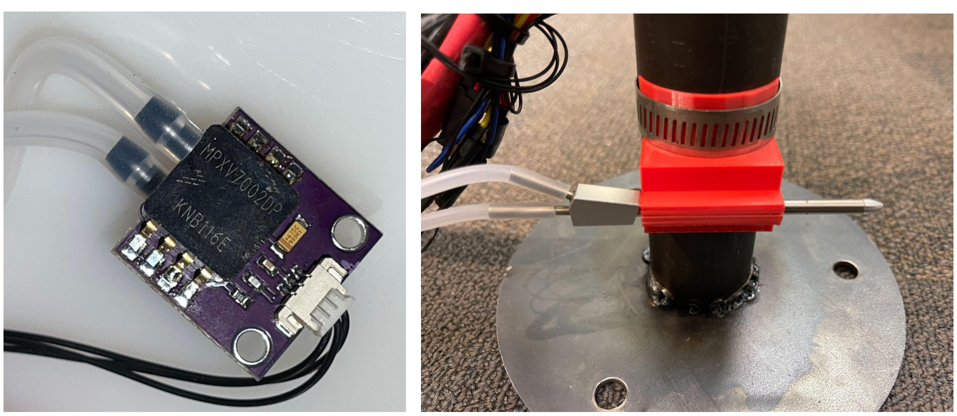

Figures 15 & 16: Analog differential pressure sensor and pitot tube

The wind speed is used in the control algorithm to set the appropriate load resistance and account for the various operating conditions of the turbine like in the rated power task where the turbine must maintain a constant power output after 11 m/s up to 14 m/s.

Generator Design

In the Fall semester, the generator was designed with a stator 8 inches in diameter and rotors that were 6.6 inches in diameter and 0.25 inches thick. The twelve magnets used with this generator were 0.5 inch thick with a diameter of 1.25 inches. It was found that this generator was significantly too large and had too much inertia, struggling to spin at 5 m/s and not reaching the RPMs desired at higher speeds. During the Spring semester, the team focused on building a smaller turbine with significantly less inertia. The new stator design has a diameter of 6.4 inches and the rotors were reduced to 5.5 inches in diameter and 1/8 inch in thickness. Additionally, the new stator windings were made with a larger trace thickness and heavier copper weight to reduce armature losses at higher currents. The magnets were also reduced to ¼ in thickness with a diameter of 1 inch. Excess material was removed wherever possible including on the inside of the rotors with a three-spoke support design, with the outside of the rotors being curved around the outside edge mirroring the magnets, and by creating lighter set screw flanges. The generator was assembled with lighter cast acrylic bearing blocks, a resized steel generator shaft, and the rotors.

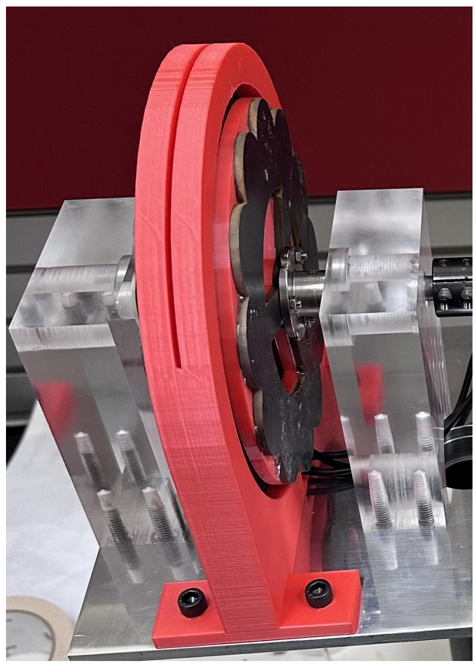

Figure 17: Axial flux permanent magnet synchronous generator from Spring semester

The new PCB stator winding resistance for a single phase was measured at 0.4809Ω, so that the armature electrical losses for the system can be accounted for. Using the TSR=3.5 blades from Qblade, the torque values were extracted at a range of wind speeds from 5-14 m/s, as well as the coefficient of power. Since speed can be calculated from the torque and theoretical power seen by the wind-swept area, rpm values were calculated for each wind speed. Using the given speed, the output AC voltage of the generator was calculated using the machine constant of the generator, which was converted to its DC equivalent. Utilizing the DC voltage output, it was predicted and verified in testing that the voltage would remain well below the operating limits of the competition (< 25V DC).

Turbine Controls

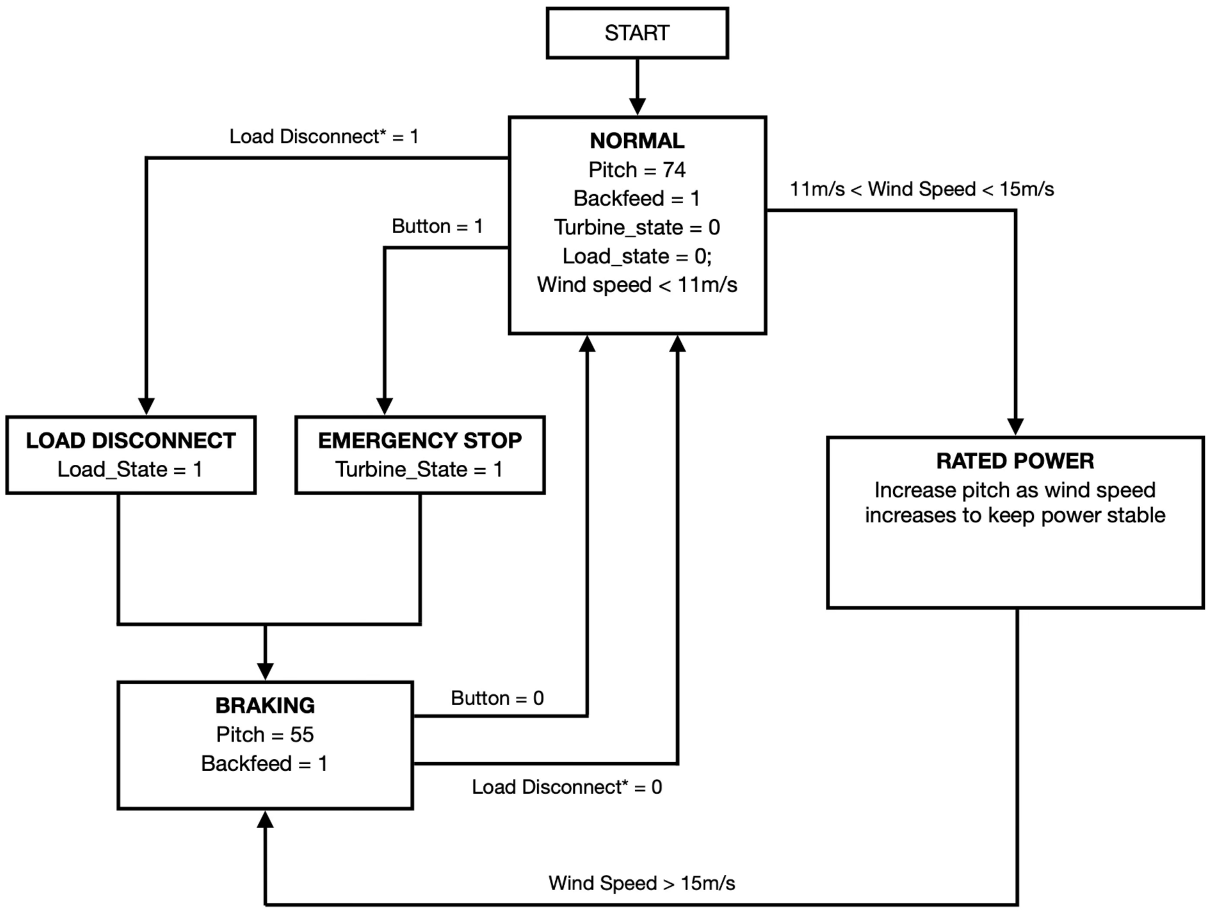

Figure 18: Turbine controls state diagram

Turbine Assembly & Installation

Turbine Assembly

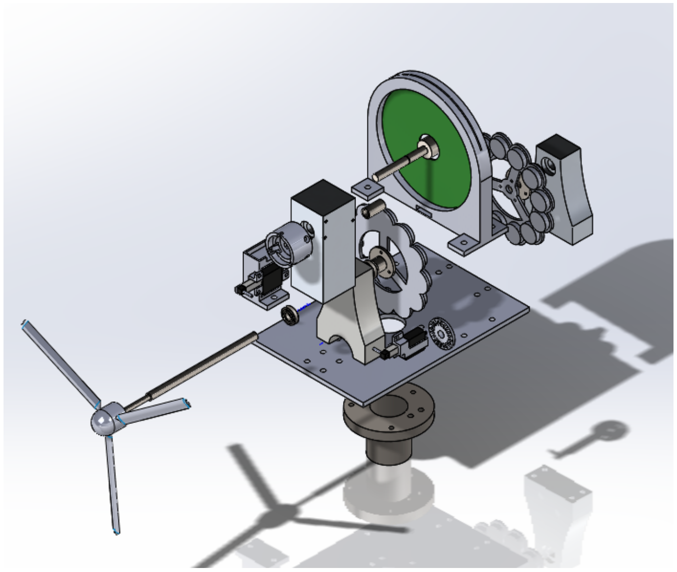

Figure 19: SOLIDWORKS subcomponents of turbine assembly

The main components involved with mounting the turbine are the bearing blocks and the baseplate. Two bearing blocks support the generator in the rear, and one supports the pitch control system and blades in the front. With the first prototype last semester, all the bearing blocks were made out of aluminum and the turbine was extremely heavy. This semester the rear generator blocks were fabricated from acrylic to reduce weight. The front bearing block was reused from last semester as it contained the actuator mounting system and was modified to fit the new shaft height associated with the new stator. The baseplate was made out ¼ inch aluminum, reduced from ½ inch last semester to also reduce weight. With mounting the bearing blocks on the baseplate, accuracy in positioning was extremely important to ensure the concentricity of the shafts to minimize friction and vibrations. This was accomplished through very precise position of the holes in the baseplate and associated threaded holes in the bottom of the bearing blocks. For the generator shaft, the same general design idea from last semester was used again with the stepped-up section to separate the rotors. For this semester, the thickness of the magnets was decreased therefore the rotors had to be moved closer together to maintain the 1mm gap between the face of the stator and the magnets. A new generator shaft was lathed to fit the new dimensions.

The generator assembly begins with installing the rotors onto the generator shaft with the stator in between. With the set screw flanges already bolted to the rotors, slip one rotor onto the shaft until it rests against the stepped-up section of the shaft, and tighten the set screw. Add a snap ring onto this side of the shaft. Bolt the middle bearing block to the baseplate with a bearing installed and slide the end of the shaft with the rotor on it through the bearing and block. With the stator already in the mount, slide the stator around the shaft and carefully guide the stator wires under the middle bearing block and down the stem hole. Bolt the stator mount to the baseplate. Slide the other rotor with a set screw flange bolted to it onto the free side of the shaft, and ensure there is a mechanism to hold the rotor and withstand its strong magnetic attraction to the other rotor so it doesn't aggressively slam into the stepped-up section of the shaft. Once the rotor is carefully installed on the shaft, tighten the rotor set screw and add a snap ring to this end of the shaft. Slide the free end of the shaft into the rear bearing block with a bearing already installed and bolt the rear block to the baseplate.

Begin the front assembly by bolting the front bearing block to the baseplate with a bearing installed. The front rotor shaft should have the rotor head and swash plate coupler already installed. Slide the front rotor shaft through the bearing and couple the rotor shaft to the generator shaft. Slide the swash plate coupler rods through the coupler and into the linear actuators. Screw the actuators to the front bearing block using the associated mounting brackets. Slide the blades into place on the rotor head and secure them with screws. Finally, place the nacelle over the turbine and bolt it to the baseplate.

Figure 20: Turbine Final Assembly without the nacelle

Commissioning Checklist

Step #	Event Description
1	Run the power and controls wires through the hole at the base of the substructure tubing, and keep ahold of the connectors when pulling to keep dry.
2	Twist the substructure into the sand with the PVC pipe C attachment inserted into the top of the substructure mounting plate. Make sure the mounting plate slots are parallel with the incident wind direction.
3	Insert a metal plate into a slot on either side of the substructure and push it down with the PVC pushing tool.
4	Install competition-provided transition stub by sliding it over the top tube of the substructure and screwing down the bolts
5	Maneuver the turbine into the wind tunnel and connect the wire connectors that come from the turbine tower stem to the wires that are fed up through the substructure–feeding the wires up by pushing from the bottom.
6	Lower the turbine down onto the mounting flange and lock down nuts over the tri-screw mounting flange.
7	Attach the 3 wire connectors coming from the turbine to their respective receiving cables coming from the glands on the turbine-side electrical enclosure.
8	Plug in the JST connector from the turbine-side electrical enclosure to the PCC.
9	Connect the DC output of the turbine-side enclosure to the PCC input using the Anderson power pole terminated red/black cables.
10	Connect the DC output of the PCC to the load-side enclosure input using the Anderson power pole terminated red/black cables.
11	Connect the 120VAC to 15V DC converter into the wall power and plug in the Anderson power pole connector to the labeled 15V input gland for the load-side electronics enclosure.
12	Ensure all connections are secure and the lids of the electrical enclosure are securely fastened.

Turbine Testing & Results

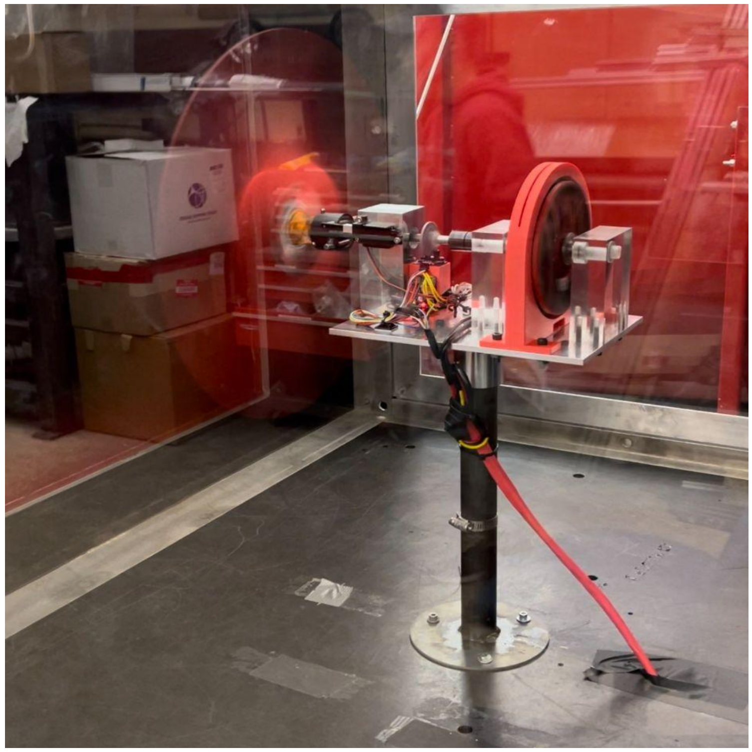

Figure 21: Turbine testing in the UW-Madison closed-loop wind tunnel

Testing of the turbine revolved around two variables: pitch and load resistance control. Through data from Qblade regarding speeds and torque along with electrical specifications of the generator, theoretical values for resistance loads were determined. These calculations were performed in excel and are shown below.

WORTMANN FX 60-126 AIRFOIL (TSR=3.5) NEW GENERATOR

Wind Speed (m/s)	Max Available Power w/ Cp(W)	Input Torque (N-m)	RPM	Shaft Speed (Rad/s)	Peak Phase Voltage (V-LN)	DC Voltage Out (V)	Current Required (A)	Resistance Required	Generator Power (W)	Generator Power (W) w/ Armature Loss	Power Delta (IN-OUT)	Efficiency
5	4.83875	0.061	757.4864816	79.32377049	11.42420943	9.447821195	0.51215512	18.44718684	4.83875	4.712608551	0	97.39309845
6	8.36136	0.089	897.1363489	93.94786517	13.53037154	11.18961726	0.747242716	14.97454177	8.36136	8.09283906	0	96.78854948
7	13.27753	0.12	1056.592644	110.6460833	15.93524892	13.17845086	1.007518269	13.08011106	13.27753	12.78937175	0	96.32342571
8	19.81952	0.16	1182.89089	123.872	17.84004544	14.75371758	1.343357692	10.98271716	19.81952	18.9516831	0	95.62130215
9	28.21959	0.2	1347.386654	141.09795	20.32092676	16.80540643	1.679197115	10.00800101	28.21959	26.86359485	0	95.19484461
10	38.71	0.246	1502.65611	157.3577236	22.66265935	18.74201928	2.065412452	9.074225956	38.71	36.65851494	0	94.70037442
11	51.52301	0.3	1640.028931	171.7433667	24.73447967	20.45541468	2.518795673	8.121109189	51.52301	48.47202091	0	94.0783951
12	66.89088	0.354	1804.409832	188.9572881	27.21362864	22.50567088	2.972178894	7.572111802	66.89088	62.6426828	0	93.64906366
13	85.04587	0.421	1929.046381	202.0091924	29.09336389	24.06021194	3.534709928	6.806841983	85.04587	79.03742159	0	92.93504975
14	106.22024	0.483	2100.059913	219.9176812	31.67254444	26.19319425	4.055261034	6.459064912	106.22024	98.31177119	0	92.55464984

Figure 22: Turbine load calculations with TSR=3.5 blades

The team used these as base values to test the pitch. The team varied the pitch along the path of actuation at each speed with the specific theoretical load at the speed. A power versus pitch control diagram was created which can be seen below, and it was found that the optimal pitch angle was practically constant for wind speeds from 5 m/s to 11 m/s.

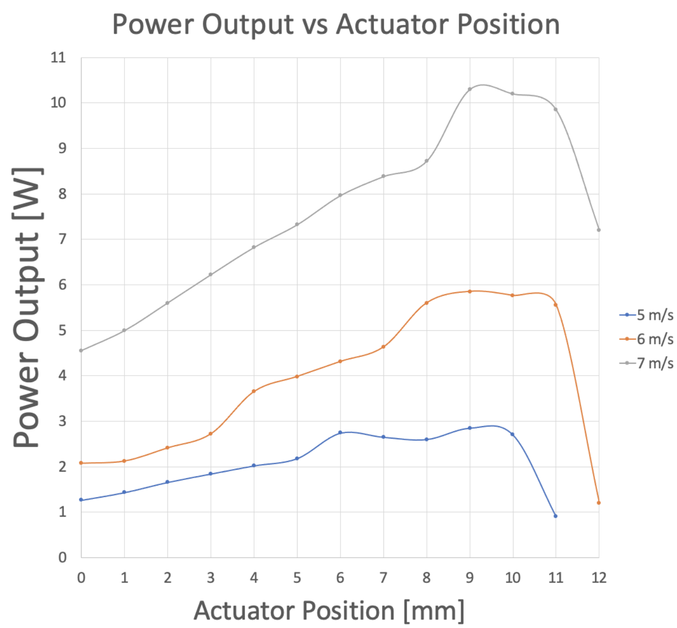

Figure 23: Power versus pitch angle at various wind speeds

Once the optimal pitch angle was found, the team went back and verified that the theoretical load values were the actual optimal values by varying the load at the optimal pitch angle, and the theoretical values resulted in being true. A power curve was then produced using the optimal pitch and load values which can be seen below.

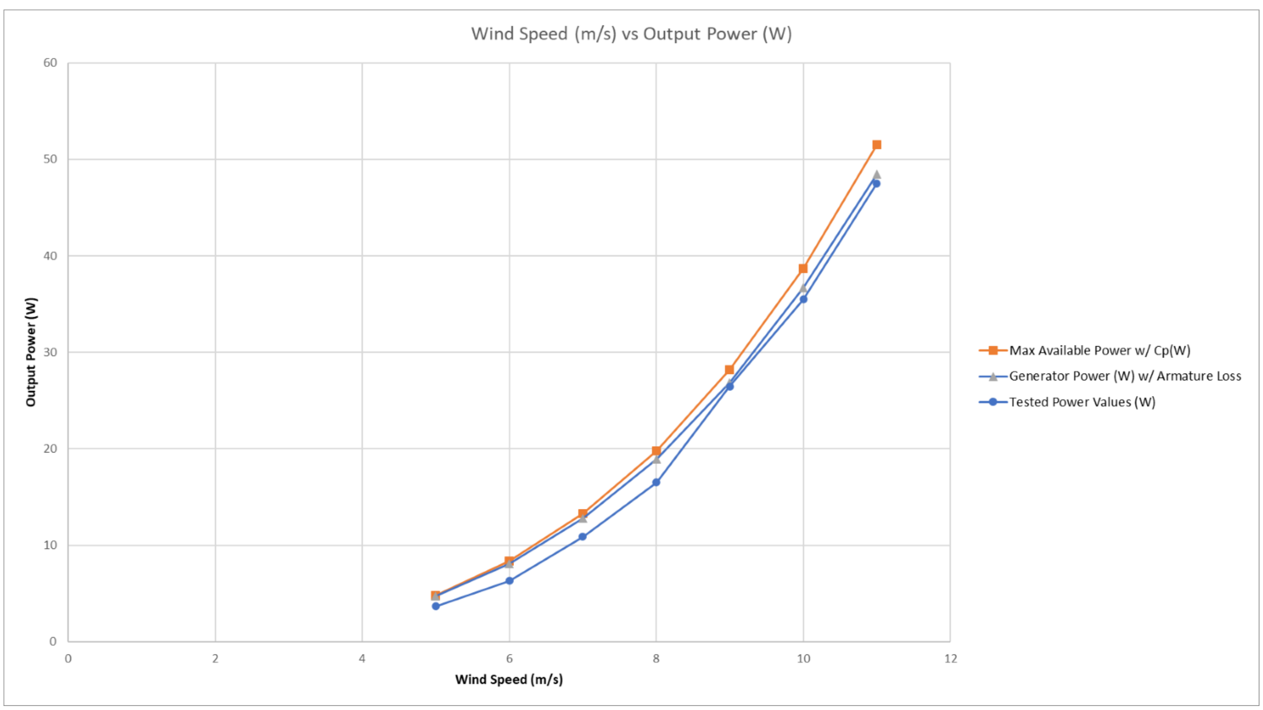

Figure 24: Power versus wind speed testing data